A Physics-Specific Change Point Detection Method Using Torque Signals in Pipe Tightening Processes

Juan Du, *Member, IEEE*, Xi Zhang, *Member, IEEE*, and Jianjun Shi

***Abstract*— Change point detection in torque signals has widely been adopted for quality inspection during pipe tightening processes. Previous studies on the change point detection in this process generally focus on directly detecting the change points throughout torques without considering the underlying mechanism that generates various quasi-periodic nonlinear profiles, thereby introducing a series of false change points and increasing the risk of releasing defective pipes. To overcome this problem, we propose a novel change-point detection approach by fully considering the profile generating mechanism, and introduce a similarity-weighted matrix with an integration of dynamic time warping and tightening physics. Thus, the probability of false detection of change points is reduced. A weighted regression model is developed to determine the authentic change points by introducing the tightening process constraints. The performance of the proposed approach is demonstrated by both numerical and real case studies, and results show that the proposed method achieves a more effective detection power than the other existing methods in the pipe tightening processes.**

***Note to Practitioners*—This paper was motivated by the real industrial needs of change point detection in torque signals during pipe tightening processes. Identifying the change points that substantially captures the tightening process conditions, and thus assuring the quality of pipe connections, is of great practical interest. A key challenge to this problem is that multiple uncertainties exist in the pipe tightening process, thereby leading to various nonlinear profiles with different lengths in torque signal. This fact introduces a number of fake change points and consequently mixes with the real change points regarding the process conditions. To address this issue, we propose to generate a "physical basis function" to adaptively assign the weights to those nonlinear profiles that may produce the fake points, by using dynamic time warping. To better use this method for change point detection, two factors should be noted: 1) the generated basis function should fully comply with the process physics and 2) this method can be widely used in torque signals with different lengths and multiple nonlinear profiles.**

***Index Terms*— Change point detection, dynamic time warping, pipe tightening processes, process monitoring, weighted regression.**

I. Introduction

IN A production line, a single working process is usually designed with a series of critical phases to satisfy product functional requirements. For example, pipe tightening processes have three phases, namely, thread engagement, metal surface sealing, and shoulder contact [1], which sequentially and collectively form the whole tightening procedure. Any violation to the process criteria under each phase might result in serious product malfunction (e.g., leaking or loosing) or even safety problems [2]. However, in current practice, examining the product conformity is mainly conducted by offline inspection after the tightening process. This offline test has one major weakness, which may enable the ineligible products to pass through the remaining downstream processes before they can be identified by postprocess inspection, thereby leading to a large amount of waste in the production line. Furthermore, more defective pipe joints may be produced due to the delay of the offline defective joints detection.

Advancement of sensor technologies prompts the extensive use of sensor data across assembly lines. The collected sensor signals usually contain rich information that has potential to be used to quantitatively characterize the process conditions for product quality assurance. Specifically, in pipe tightening processes, the torque signal can be used for process condition monitoring by judging a pair of change point locations, which should be in the acceptable ranges according to the standards of the American Petroleum Institute (API) [24], [25]. As shown in Fig. 1, a pair of change points A and B separate the torque signal into three phases, and the torque values of these two points in an eligible connection should be simultaneously satisfied within a specified range as labeled by horizontal dashed lines; otherwise, the connection is regarded as defective. An inaccurate detection of the location of any change point may cause a failure for identifying unqualified pipe connections; these connections lead to product rework or production wastes. In practice, the postinspection such as hydrostatic testing will be the following step after the pipe connection. The successful detection of nonconforming parts via automatic change point detection during the pipe tightening process might reduce the costs of hydrostatic testing as well as the risk of nonconforming product releases. The annual loss from the failure of oil pipes reaches half a billion dollars, with two-third of these failures caused by pipe connections [3]. Therefore, a precise detection tool for change points is an

Manuscript received August 26, 2018; accepted October 21, 2018. Date of publication November 30, 2018; date of current version July 1, 2019. This paper was recommended for publication by Associate Editor J. Song and Editor L. Shi upon evaluation of the reviewers' comments. This work was partially supported by the National Natural Science Foundation of China under Grant 71690232, Grant 71471005, Grant 71571003, and Grant 61433001. *(Corresponding author: Xi Zhang.)*

J. Du and X. Zhang are with the Department of Industrial Engineering and Management, Peking University, Beijing, 100871, China (e-mail: dujuan@pku.edu.cn; xi.zhang@pku.edu.cn).

J. Shi is with the H. Milton Stewart School of Industrial and Systems Engineering, Georgia Institute of Technology, Atlanta, GA 30332 USA (e-mail: jianjun.shi@isye.gatech.edu).

Color versions of one or more of the figures in this paper are available online at http://ieeexplore.ieee.org.

Digital Object Identifier 10.1109/TASE.2018.2878961

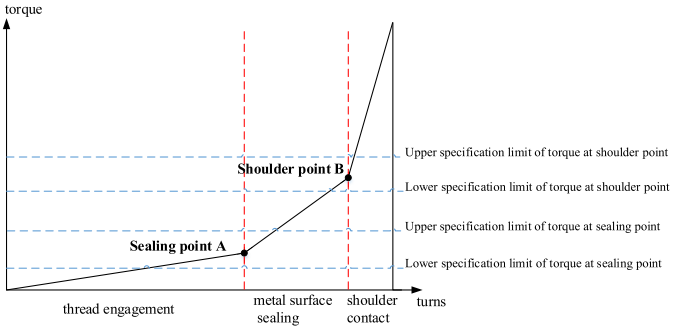

Fig. 1. Nominal torque curve in the pipe tightening process with three critical phases.

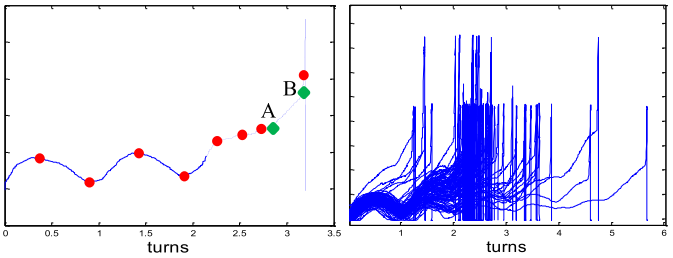

Fig. 2. Sensor toque signals in the pipe tightening process. (a) Sample of collected torque signals. (b) Samples of torque signals with varying lengths.

essential task for product quality assurance in pipe tightening processes.

However, developing such an effective tool to detect a pair of change points throughout torque signals is a challenging task because various uncertainties occur in assembly systems that are generally shown with multiple types of nonlinear profiles in torque signals. Thus, these profiles due to uncertainties would greatly affect the accuracy of the change point detection. Generally, in addition to the common measurement errors in the signal such as Gaussian noises, one type of nonlinear profile widely exists, which contains a quasi-periodic pattern with varying periods and lengths. To the best of our knowledge, this condition mainly occurs because of the inconsistency of upstream processes such as the misalignment of pipes before connection and the unstraightness of pipes, which is difficult to fully avert. Although this nonlinear profile will not alert any ineligible connection signs, the occurrence of this type of profile primarily conceals locations of change points. Fig. 2(a) depicts an example of the torque signal obtained from the real tightening process with a nonlinear profile originated from the pipe misalignment. This process produces pseudochange points (marked in dots) and sets a high barrier to directly locate the authentic change points (marked in diamonds) throughout the torque signal. Fig. 2(b) shows a batch of samples of torque signals that are collected from a single connection machine, and different lengths as well as varying nonlinear patterns due to the inconsistent preassembling processes in the upstream stage could be observed. This condition also poses another challenge to accurately locate the change points by traditional signal processing methods.

In this paper, to overcome the challenges for change point detection, we aim to eliminate the negative effect that obscures the true change points produced from this type of quasi-periodic profiles with different patterns and propose an innovative change point detection method by considering the origin of the nonlinear profiles under different signal lengths. Specifically, we consider encoding the mechanism that generates such profiles into a "physical basis function" and design a similarity-weighted matrix via dynamic time warping to quantify the similarity between the "physics" and underlying profiles in the pipe tightening process. The similarity-weighted matrix will be used to mitigate the negative effect generated by these quasi-periodic profiles in the following procedure. We first formulate the change detection problem as a sequential piecewise linear model following the physical mechanism of the pipe tightening process, and an $F_{\max}$ test is used to capture the potential change points. A selection procedure is then proposed in light of the physical constraints to shrink the set of pseudochange points. A weighted three-phase regression model is finally established by incorporating the similarity-weighted matrix to determine the true change points.

The contributions of this paper can be summarized as follows.

1) We designed the "physical basis function" from the domain knowledge to provide a measure for characterizing multiple types of nonlinear profiles that are generated from underlying latent factors of the tightening process.
2) We leveraged dynamic time warping to deal with the unequal length characteristic of sensing signals and physical basis function.
3) A similarity-weighted matrix is designed to measure the deviation of sensor torque signals from the nominal torque curve for authentic change point determination.

The rest of this paper is organized as follows. We first briefly review the topics related to change point detection in Section II. In Section III, we present our proposed methodology on change point detection. Section IV provides simulation studies and sensitivity analysis of the proposed method. In Section V, a real case study on pipe-tightening processes is provided to validate our proposed approach. Finally, conclusions are summarized in Section VI.

II. Literature Review

To ensure the quality of the connected pipes, a variety of postprocess inspection methods have been developed for quality evaluation, such as internal pressure leak detection, external pressure leak detection, thermal cycling tests, and make-up/break-out test. The detailed procedures and recommended postprocess inspection practices for pipe connection quality can be found in [4]. These tools are essential for final product inspection but are typically used when the tightening process is completed. Thus, the corrections or compensation to the inappropriate working conditions may not be implemented in a timely manner, which leads to many defective products or material wastes. Alternatively, by harnessing the in-process signals such as torque signals, developing such automatic change point detection methods for in-process quality inspection elicits extensive attention in contemporary research.

Existing change point detection methods can be generally divided into two lines of research, that is, data-driven methods

and engineering-driven methods. Data-driven methods aim to solve the change-point detection problem by statistical modeling as well as testing associated parameter changes. These methods can be further categorized into three classes. The first category conducts change point detection by identifying distribution changes in the signals. Distribution change detection methods have been developed such as likelihood ratio test methods [5], [6] or spectrum methods [7], [8]. Powerful tools in process control including various categories of control charts are conventional examples of this category. These types of methods are adoptable when the data or extracted features comply with the model assumptions or constraints. However, they are not suitable in tightening processes because variations from existing nonlinear profiles in torques will enable the distribution to change superficially, whereas the truth as regards the process condition beneath the profiles is fixed. Consequently, a series of pseudochange points will be selected. The second category detects the change points by identifying the changes of state variables in the established models. These methods usually characterize the process condition by using a state-space model and developing state estimation algorithms to identify the changes. For example, the second-order polynomial state-space model is proposed for endpoint detection in the semiconductor manufacturing process [9]. These methods are more effective when the collected temporal data originates from a discrete or discretized state space in which the finite state transits following a definite pattern [10]. However, in a complex manufacturing process, state variables and corresponding transition patterns may not always be known. In addition, precise estimation of state variables may not be obtained from signals with a variety of nonlinear profiles. For example, the torque signals with quasi-periodic profiles may cause an incorrect estimation of phase changes during pipe tightening processes. The third category is signal-segment-based approaches. These methods define signal segmentation parameters in the model as the location of change points to characterize process changes. These methods are successfully implemented in this paper for mean shift change point detection. For instance, a piecewise constant model is established to detect multiple change points by testing the mean of a new sequence with the old one [11]. Moreover, analysis based on maximization of likelihood [12] or marginal-likelihood [13] function of the segmented data is proposed to estimate change points. The major limitation of existing segmented methods is that the assumption of signal pattern is stepwise signal. However, sensor signals from numerous manufacturing processes may not be stepwise signals, such as torque signals. Therefore, existing pure data-driven methods cannot be directly adopted for change point detection in the tightening process.

Engineering-driven methods incorporate engineering domain knowledge of manufacturing process into statistical modeling for change point detection. Such methods have been successfully applied in many manufacturing processes, including nanomanufacturing process [14] and progressive stamping process [15]. Specifically in the tightening process, two empirical methods are developed for shoulder point detection by considering the piecewise linear structure of the nominal torque curve. These two empirical methods use simple "derivative" of torque curve to calculate the slope of the segment piece and set a threshold for shoulder point identification [2], [16]. However, these methods occasionally identify false change points because the collected torque signals consistently have multiple nonlinear profiles. In addition, these two methods can only identify shoulder point. To address these problems, in our previous work, a sequential piecewise linear model was proposed by considering the linear relationship between screwing turns and torques based on the principle of elastic mechanics [17]. To provide a more accurate detection result, a three-phase state-space model was developed for the pairwise change point detection by investigating the phase changes during the tightening process [18]. These two methods show a satisfactory detection power on the torque signals with few simple nonlinear profiles (e.g., a single quasi-periodic profile exists in the torque). However, they cannot effectively identify multiple change points in torque signals with various nonlinear profiles (e.g., multiple quasi-periodic profiles with varying periods and lengths) because of the lack of complete investigation in the generation mechanism of signal profiles. Therefore, the existing engineering-driven methods cannot meet the requirements of multiple change point detection when different types of nonlinear profiles exist in torque signals. It is desirable to develop an alternative approach that considers the generation mechanism of signal profiles and mitigates the negative effect of quasi-periodic profile for change point detection in the tightening process.

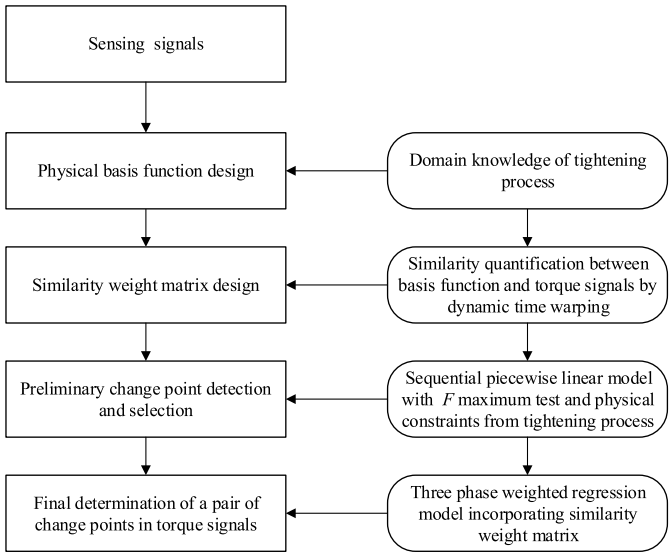

Fig. 3. Framework of the proposed methodology.

III. Research Methodology

A. Overview

Fig. 3 shows the framework of the proposed method. Based on the physical analysis of nonlinear patterns in torque signals, the "physical basis function" is first designed to capture the nonlinear patterns of torque signals. Considering the varying

periods of the nonlinear patterns and lengths of the signal pieces, we adopt dynamic time warping to measure the similarity between torque signals and "physical basis function" to provide a similarity-weighted matrix. A pool of potential change points can be identified by the developed sequential change point detection and selection method. A weighted three-phase regression model is finally proposed to obtain a pair of change points from this potential change point pool by incorporating the similarity-weighted matrix derived from the dynamic time warping.

Based on the fundamental physical analysis [19], [20] of torque signals during tightening processes, a three piecewise linear curve, with a pair of change points, could fully represent the three-phase pipe tightening, as shown in Fig. 1. Thus, guided by physical interpretations, the basic assumption in this paper is that a pair of change points coexists within the torque signal, and consequently three segments exist.

The remainder of this paper is organized as follows. Section III-B provides details on the "physical basis function" and similarity-weighted matrix generated through a dynamic time warping method. Section III-C presents the details on acquiring a set of potential change points through the established prior information from the similarity-weighted matrix. This section also serves as the input for the optimal pair of change points in Section III-D.

B. "Physical Basis Function" and Similarity-Weighted Matrix Design

Given a variety of latent factors including misalignment and unstraightness in the tightening process, quasi-periodic profile in the torque signal frequently emerges with varying periodic lengths. This underlying pattern can be characterized by a physical function, and by using such a function, this type of nonlinear pattern is expected to be fully characterized. Considering the varying lengths of the quasi-periodic profiles and length of the torque signal, the static physical function is incapable of capturing all patterns generated by those latent factors. To efficiently evaluate the similarity between such profiles and the designed physical function, dynamic time warping is adopted to measure the distance between torque signals and "physical basis function."

Dynamic time warping [26] is initially designed for time-series similarity measurement by aligning two time series with the minimum mapping distance. The major advantage of dynamic time warping over traditional distance calculation is that the lengths of two series applied by this technique may vary. The details of dynamic time warping are provided in the Appendix.

Multiple quasi-periodic profiles mainly exist in the thread engagement phase, and certain nonlinear profiles cause the accurate change-point detection to be challenging. To mitigate the negative effect generated by these quasi-periodic profiles to avoid the false detection of change points, we propose the "physical basis function" to capture the quasi-periodic patterns of torque signals. Specifically, the warping distance $D_i (i = 1, \ldots, N)$ between the "physical basis function" and torque series from the first torque point ($i = 1$) to the ith($i = 1, \ldots, N$) torque point is sequentially calculated by dynamic time warping to quantify the influence of the quasi-periodic patterns. Here, N is the time index that corresponds to the maximum torque of the signal. The warping distance characterizes the similarity between the "physical basis function" and torque signals, and the large distance indicates that the corresponding torque sequence is not inclined to match the quasi-periodic pattern. The small distance indicates the similarity to the quasi-periodic patterns and is slightly important for change-point detection. The shortest warping distance indicates that the torque signals consist of quasi-periodical patterns that mainly occur in a thread engagement phase in the tightening process. The two change points are located behind the engagement phase, which introduces the prior information for the subsequent sequential change-point detection in Section III-C. Thus, the sequential warping distances between the "physical basis function" and torque sequences can be regarded as a similarity-weighted matrix, that is, $\boldsymbol{S} = \text{diag}(D_i), i = 1, \ldots, N$, which can be used for the final change-point detection described in Section III-D.

C. Sequential Change Point Detection and Selection

Given the model assumption that the torque curve is piecewise linear and the change point is located at the slope change of two sequential linear segments, a two-phase regression model is proposed for potential change point detection, as follows:

$$y_k = \begin{cases} \alpha_1 + \beta_1 x_k + \varepsilon_k & 0 \le x_k \le c_0 \\ \alpha_2 + \beta_2 x_k + \varepsilon_k & c_0 < x_k \le x_N \end{cases} \tag{1}$$

where x_k, y_k, and ε_k represent screwing turn observation, torque observation, and Gaussian noise at time k, respectively. Parameter c_0 denotes the location of potential change point in x-axis (screwing turns) in which the slope experiences a significant change; (α_i, β_i) is the coefficient of the two-phase regression ($i = 1, 2$); and x_N is the turn that corresponds to the maximal torque of the torque signal.

Based on the two-phase regression model, the detection of the potential change points is converted into the detection of the slope change, that is, $\beta_1 \neq \beta_2$. Thus, the null hypothesis is $H_0 : \beta_1 = \beta_2$, $\alpha_1 = \alpha_2$. The F_0 statistic for change time $K_0 \in \{1, \ldots, N\}$ can be used for the following hypothesis test:

$$F_0 = \frac{(\text{SSE}_0 - \text{SSE}_1)/2}{\text{SSE}_1/(N-4)}, \tag{2}$$

where

$$\text{SSE}_0 = \sum_{k=1}^{N} (y_k - \alpha_0 - \beta_0 x_k)^2, \quad \alpha_1 = \alpha_2 = \alpha_0, \quad \beta_1 = \beta_2 = \beta_0 \tag{3}$$

$$\text{SSE}_1 = \sum_{k=1}^{K_0} (y_k - \alpha_1 - \beta_1 x_k)^2 + \sum_{k=K_0+1}^{N} (y_k - \alpha_2 - \beta_2 x_k)^2. \tag{4}$$

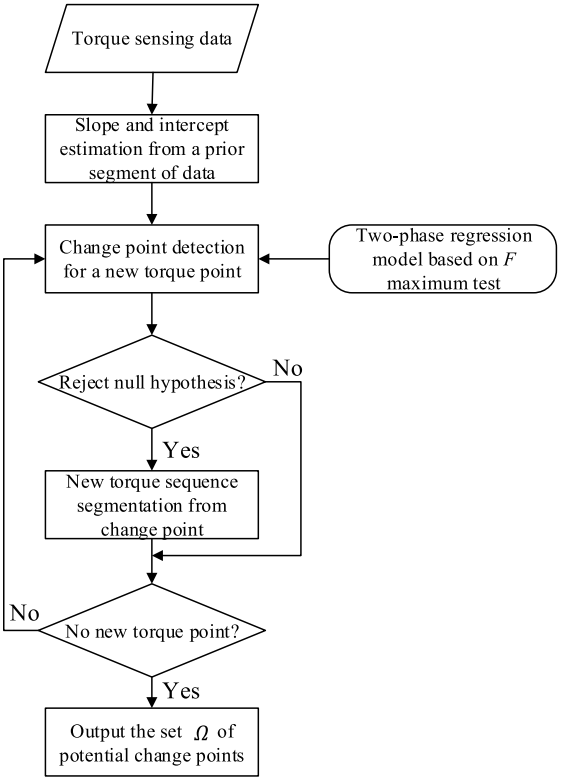

Fig. 4. Flowchart of sequential change point detection.

The parameters in (3) and (4) can be estimated from the least squares. The inference of K_0 is provided by

$$F_{\max} = \max_{1 \le K_0 \le N} F_0. \tag{5}$$

In practice, $F_{\max}$ is obtained by searching throughout the torque signal to determine the point that maximizes F_0. For example, the $F_{\max}$ percentile can be borrowed to test the significance of the statistic [21].

The traditional $F_{\max}$ test for two-phase regression model can only detect one change point for a given sequence. Considering that the number of the potential change points is unknown, we develop a sequential change point detection method to identify all potential change points based on the two-phase regression model and $F_{\max}$ test. The flowchart of our proposed sequential change point detection is shown in Fig. 4. The prior information from Section III-B provides the initial point where the sequential change-point detection begins. The slope and intercept are first estimated on the basis of the torque sequence from the first point to the initial point. Potential change points are sequentially identified by using the $F_{\max}$ test when subsequent sampled torque points are obtained. The torque sequence is segmented at the point where the corresponding $F_{\max}$ statistic is significant at the specific confidence level. This procedure is repeated until all torque points before the points at the maximal torque are tested. Therefore, the number of two-phase regressions is equal to the number of torque points starting from the initial point obtained from Section III-B to the point with the maximal torque. A change point set Ω, which includes all the potential change points of the torque signals, can be finally obtained after this procedure.

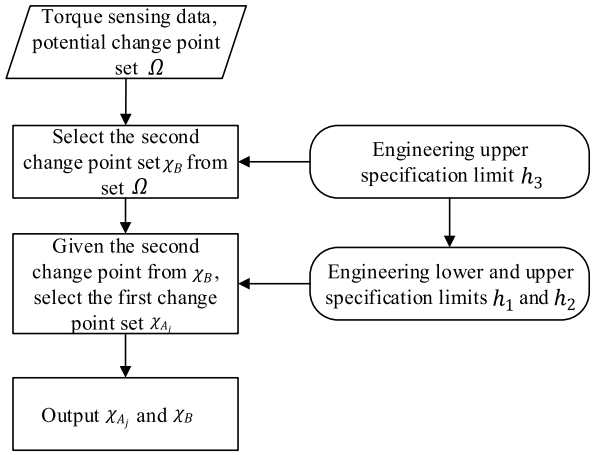

Fig. 5. Flowchart for change point selection procedure.

To achieve in-process change point detection, the pool of potential change points can be shrunk by studying the process in an engineering design perspective. Specifically, in the tightening process, upper and lower specification limits from engineering design can be considered to obtain a shrunken set of potential change points. On one hand, a designed lower and upper specification limits h_1 and h_2 of screwing turn distance occurs between two change points A and B (Fig. 2), thereby indicating that the screwing turn distance between these two change points is larger than h_1 and smaller than h_2. On the other hand, an upper specification limit h_3 exists on the deformation of shoulder contact, thereby indicating that the screwing turn distance between the second change point and the point at the maximal torque value is smaller than h_3. We set a zero lower limit for the second change-point detection because the location of the second change point is near the point with the maximum torque, and the physical turn distance is relatively short in the shoulder contact phase. In practice, the engineering specification limits h_1, h_2, and h_3 can be obtained from the product design phase.

The flowchart of the change point selection based on the engineering geometric constraints is shown in Fig. 5. The selection approach gives two smaller potential change point sets χ_{A_j} and χ_B for the first change point and the second change point, respectively,

$$\chi_{A_j} = \{c_i | h_1 \le c_j - c_i \le h_2, c_j \in \chi_B, c_i \in \Omega\}, \quad j = 1, 2, \ldots, M \tag{6}$$

$$\chi_B = \{c_j \mid 0 < x_N - c_j < h_3, c_j \in \Omega\} \tag{7}$$

where M is the number of points in χ_B set. c_i and c_j denote the locations of one potential first and second change points in x-axis (screwing turns). Given one potential second change point c_j in χ_B, a set χ_{A_j} exists, which contains the corresponding potential first change points. Thus, a final determination is needed to determine the optimal combinations of a pair of change points in torque signals.

D. Determination of Pair of Change Points

The nominal torque curve under the torque signal from a physical mechanism analysis is piecewise linear. Owing to the pool of potential change points, we must select the optimal points along the collected torque signals on the basis of the estimated nominal piecewise linear curves. To achieve this process, we estimate the slope and intercept by minimizing weighted least squares, that is, weighted residual sum of squares, where the weight is obtained from the dynamic time warping distance.

According to the model assumption, a pair of change points segments the torque signals into three pieces, and the torque value beneath each piece should be proportional to the screwing turns. Thus, a three piecewise linear regression model can be built to characterize the pipe tightening process

$$y_k = \begin{cases} a_1 + b_1 x_k + e_1 & 0 \le x_k \le c_1 \\ a_2 + b_2 x_k + e_2 & c_1 < x_k \le c_2 \\ a_3 + b_3 x_k + e_3 & c_2 < x_k \le x_N \end{cases}, \tag{8}$$

where c_1 and c_2 denote the locations of the first and the second change points in the x-axis (screwing turns) and $e_i (i = 1, 2, 3)$ is Gaussian noise. The identified change point must be on the observed torque signals based on the API regulation. Thus, we ignore the constraint in which the segments are connected at the identified change points. The change points can be determined by minimizing the following weighted residual sum of squares:

$$\min_{c_1, c_2} \ \text{MWRSS}, \tag{9}$$

$$\text{s.t. } c_1 \in \chi_{A_j}, \quad c_2 \in \chi_B, \ \forall j = 1, 2, \ldots, M. \tag{10}$$

Here

$$\begin{aligned} \text{MWRSS} &= \min_{a_i, b_i} \text{WRSS}, \quad i = 1, 2, 3, \\ \text{WRSS} &= \sum_{k=1}^{K_1} \omega_k (y_k - a_1 - b_1 x_k)^2 \\ &\quad + \sum_{k=K_1+1}^{K_2} \omega_k (y_k - a_2 - b_2 x_k)^2 \\ &\quad + \sum_{k=K_2+1}^{N} \omega_k (y_k - a_3 - b_3 x_k)^2, \end{aligned} \tag{11}$$

where ω_k is the weight of the torque point at time k, and K_1 and K_2 are the sampling points that correspond to c_1 and c_2. The proposed similarity-weighted matrix $\boldsymbol{S}$ in Section III-B implies that the underlying quasi-periodic patterns in torque signals can be adopted as the weight matrix, thereby indicating that ω_k is proportional to the warping distance D_k, and $\sum_{k=1}^{n} \omega_k = 1$.

Given a potential second change point $c_2 \in \chi_B$, and the corresponding first change point $c_1 \in \chi_{A_j}$, the coefficient $\boldsymbol{\lambda}_i = (a_i, b_i)$ can be estimated by $\hat{\lambda}_i = (\boldsymbol{X}_i^T \boldsymbol{W}_i \boldsymbol{X}_i)^{-1} \boldsymbol{X}_i^T \boldsymbol{W}_i \boldsymbol{Y}_i, i = 1, 2, 3$. The derivation of $\hat{\lambda}_i$ can be found in the Appendix. Once $\hat{\lambda}_i$ is obtained, the MWRSS can be calculated. The pair of change points is finally determined by minimizing MWRSS. The flowchart of the determination of change points is shown in Fig. 6.

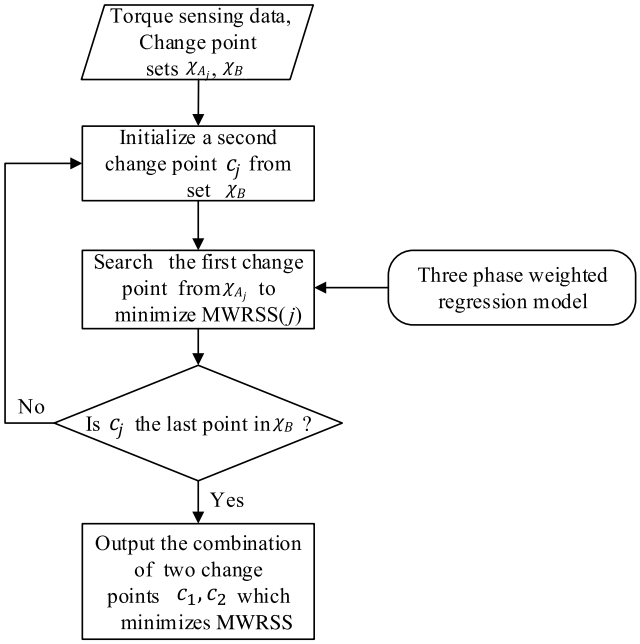

Fig. 6. Flowchart for final determination of change points.

IV. Simulation Studies

In this section, our change point detection method is validated from both numerical studies and sensitivity analysis. To implement the proposed method, "physical basis function" $g(x)$ should be first investigated. Here, we use $g(x)$ as a sinusoidal function with one cycle of screwing turn by considering pipe misalignment to mitigate the negative effect induced by the quasi-periodic pattern for a precise change point detection. The peak of $g(x)$ is the signal amplitude in the first screwing turn period.

A. Numerical Studies

In the numerical studies, signals are generated from different nonlinear functions and noises. Based on our model assumption, the torque signal is piecewise linear with a pair of change points. Thus, piecewise linear function should be chosen as the main function. Based on this piecewise linear function, three other oscillating functions are superposed, namely, sine function, sawtooth function, and sampling function, as shown in Table I.

In the tightening process, we have limited knowledge of the system operating status. Thus, in the simulation section, we simulate different types of noises to emulate the tightening system. According to [27], time series model can be used to mimic the manufacturing system, so we use autoregressive models, namely, no autocorrelation [AR(0)], first-order autoregressive correlation [AR(1)] and second-order autoregressive correlation [AR(2)] in simulation studies, as shown in Table II. Meanwhile, such simulation studies are also widely used in current literature, such as [28] and [29].

TABLE I
FOUR TYPES OF SIGNALS USED FOR NUMERICAL STUDY

Signal	Function for y_k
Piecewise linear	$y_k = \begin{cases} \frac{E_1 k}{T_1}, & k = 1, \ldots, T_1 \\ \frac{E_2 - E_1}{T_2 - T_1}(k - T_1) + E_1, & k = T_1 + 1, \ldots, T_2 \\ \frac{E_3 - E_2}{T - T_2}(k - T_2) + E_2, & k = T_2 + 1, \ldots, T_3 \end{cases}$
Sine+ Piecewise linear	$y_k = \begin{cases} \frac{E_1 k}{T_1} + z_1(k), & k = 1, \ldots, T_1 \\ \frac{E_2 - E_1}{T_2 - T_1}(k - T_1) + E_1 + z_1(T_1), & k = T_1 + 1, \ldots, T_2 \\ \frac{E_3 - E_2}{T - T_2}(k - T_2) + E_2 + z_1(T_1), & k = T_2 + 1, \ldots, T_3 \end{cases}$ $z_1(k) = E_4 \left\lvert \sin(\omega_1 \pi(\frac{k}{T_1} + E_5)) \right\rvert + E_6 \left\lvert \sin(\omega_2 \pi(\frac{k}{T_1} + E_7)) \right\rvert$
Sawtooth+ Piecewise linear	$y_k = \begin{cases} \frac{E_1 k}{T_1} + z_2(k), & k = 1, \ldots, T_1 \\ \frac{E_2 - E_1}{T_2 - T_1}(k - T_1) + E_1 + z_2(T_1), & k = T_1 + 1, \ldots, T_2 \\ \frac{E_3 - E_2}{T - T_2}(k - T_2) + E_2 + z_2(T_1), & k = T_2 + 1, \ldots, T_3 \end{cases}$ $z_2(k) = E_8 \left\lvert \text{saw}(\omega_3 \pi \left(\frac{k}{T_2} + E_9\right)) \right\rvert$
Sampling+ Piecewise linear	$y_k = \begin{cases} \frac{E_1 k}{T_1} + z_3(k), & k = 1, \ldots, T_1 \\ \frac{E_2 - E_1}{T_2 - T_1}(k - T_1) + E_1 + z_3(T_1), & k = T_1 + 1, \ldots, T_2 \\ \frac{E_3 - E_2}{T - T_2}(k - T_2) + E_2 + z_3(T_1), & k = T_2 + 1, \ldots, T_3 \end{cases}$ $z_3(k) = E_{10} \text{Sa}(\omega_4 \frac{k}{T_1} + E_{11})$

TABLE II
THREE TYPES OF CORRELATED NOISES AND RELATED PARAMETERS

Noise Type	Formulae	Parameters
AR(0)	$\phi_k = \epsilon$	$\epsilon \sim N(0, \sigma_2^2)$
AR(1)	$\phi_k = \epsilon + m_1 \phi_{k-1}$	$m_1 = 0.05$
AR(2)	$\phi_k = \epsilon + m_2 \phi_{k-1} + m_3 \phi_{k-2}$	$m_2 = -0.25, m_3 = 0.5$

In accordance with engineering practice, we generate the signal of x_k with noise via the following formula:

$$x_k = \begin{cases} \frac{E_{12} k}{T_4} + \varepsilon, & k = 1, \ldots, T_4 \\ \frac{E_{13} - E_{12}}{T - T_3}(k - T_4) + E_{12} + \varepsilon, & k = T_4 + 1, \ldots, T_3 \end{cases}$$
$$\varepsilon \sim N(0, \sigma_1^2) \tag{12}$$

where E_i, $i = 1, 2, \ldots, 13$, is a scaling parameter. We set the parameters $T_1 = 350, T_2 = 450, T_3 = 500$, $T_4 = 350$, $\sigma_1 = 70$, and $\sigma_2 = 0.005$ in our numerical study. $E_1 = 300, E_2 = 800$, and $E_3 = 2000$ are set for the main piecewise linear function. $E_4 = 300$, $E_5 = 0, E_6 = 200, E_7 = 0$, $\omega_1 = 3$, and $\omega_2 = 1.75$ are set for the sinusoidal function. $E_8 = 300, E_9 = 0.07$, and $\omega_3 = 6$ are set for the sawtooth function. $E_{10} = 300$, $E_{11} = -5$, and $\omega_4 = 10$ are set for the sampling function. $E_{12} = 2$ and $E_{13} = 2.5$ are set for x_k. Other model parameters are set as $h_1 = 0.2$, $h_2 = 2$, and $h_3 = 0.2$. To achieve a small type I error of $F_{\max}$ test of change point detection in Section III-C, the significance level is set as 0.01.

TABLE III
SDR (%) AND SDEs FOR FIRST AND SECOND CHANGE POINTS

Signal		**SDR** (%)			**SDE**	
		c_1	c_2	c_1 & c_2	SDE_1	SDE_2 ($\times 10^{-4}$)
Piecewise linear	AR(0)	93.00	98.00	91.67	0.0033	4.1551
	AR(1)	92.33	99.33	91.67	0.0033	3.7571
	AR(2)	91.33	98.67	90.33	0.0042	4.5405
Sine+ Piecewise linear	AR(0)	93.67	98.00	91.67	0.0033	4.2020
	AR(1)	92.67	97.00	90.67	0.0126	6.1383
	AR(2)	95.67	97.33	93.76	0.0116	6.0585
Sawtooth+ Piecewise linear	AR(0)	99.67	98.33	98.00	0.0012	4.5133
	AR(1)	99.00	98.67	97.67	0.0014	4.1712
	AR(2)	99.67	97.00	96.67	0.0058	4.7110
Sampling+ Piecewise linear	AR(0)	95.33	97.67	93.00	0.0025	4.2521
	AR(1)	97.33	97.00	94.67	0.0025	4.4022
	AR(2)	94.33	97.33	92.00	0.0050	5.2568

A total of 300 replications are generated for each type of signal under three different noise correlations. Fig. 7 shows the detection results from a number of typical examples. The true locations of change points in the x-axis are $c_1 = 2.00$ and $c_2 = 2.33$, respectively. The points marked by stars are the two change points identified by our proposed method, and all the change points have been successfully determined with minor differences.

To further evaluate the detection power of our proposed method, we define the range of x_k to be $[-0.1, 0.1]$ and $[-0.05, 0.05]$ as the criterion for the successful detection by considering the engineering requirements, thereby indicating that the tolerances of the successful detections of the change points should be within the given ranges. The successful detection rate (SDR) is defined as the percentage of successfully detected samples over the entire testing samples. To measure the differences between the detected locations of change points by our proposed method and authentic change point locations, we define the standard detection error (SDE) as

$$\text{SDE}_i = \sqrt{\frac{1}{N} \sum_{i=1}^{N} (\hat{c}_i - c_i)^2} i = 1, 2. \tag{13}$$

The SDR and SDEs of the detected two change points by our proposed algorithm are listed in Table III. As shown Table III, our proposed method achieves an effective detection power in terms of SDR and SDE. Although we use the sine function as the "physical basis function," the detection remains powerful for the nonsine function and multiple sine function combinations.

B. Sensitivity Analysis

Without loss of generality, as one type of factor that induces quasi-periodic profiles, pipe misalignment is considered for this sensitivity analysis. Equation (14) is established to characterize the profiles of torque signals caused by pipe misalignment in the threaded engagement phase, which contains both the quasi-periodic pattern and linear trend between turns x_k

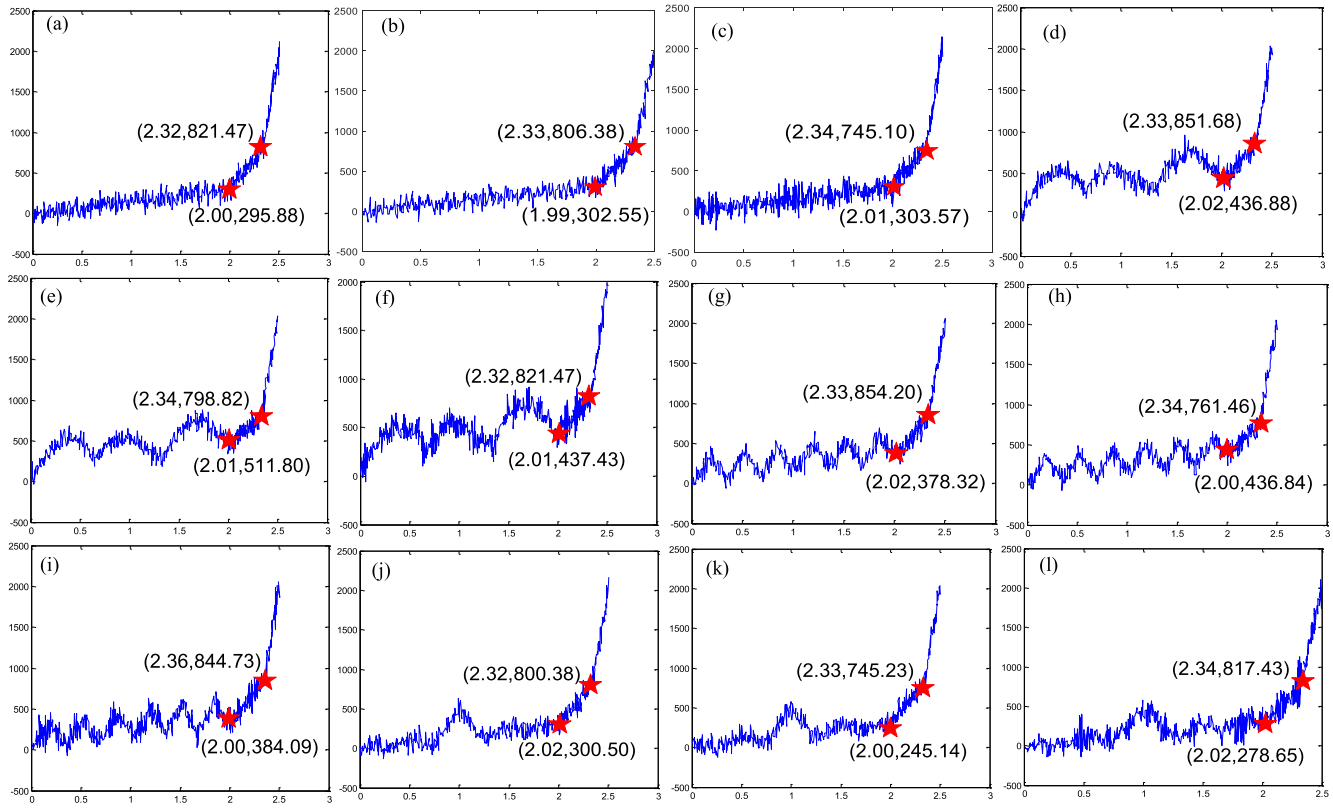

Fig. 7. Some change point detection results by our proposed method. Piecewise linear function with (a) AR(0) noise, (b) AR(1) noise, and (c) AR(2) noise. Combination of piecewise linear function and sine function with (d) AR(0) noise, (e) AR(1) noise, and (f) AR(2) noise. Combination of piecewise linear function and sawtooth function with (g) AR(0) noise, (h) AR(1) noise, and (i) AR(2) noise. Combination of piecewise linear function and sampling function with (j) AR(0) noise, (k) AR(1) noise, and (l) AR(2) noise.

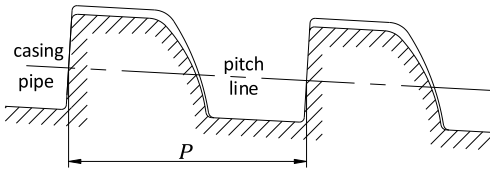

Fig. 8. Schematic of thread engagement structure.

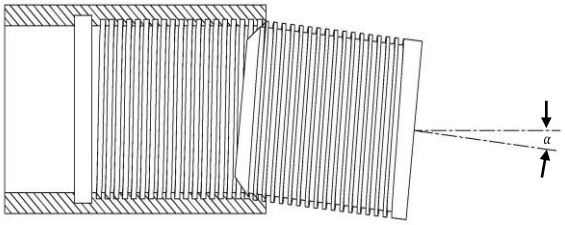

Fig. 9. Schematic of pipe misalignment.

and torques $h(x_k)$

$$h(x_k) = s_1(x_k \times P \times T + s \times f(\alpha) \times T \times P \times |\sin(x_k \times \pi)|) \tag{14}$$

where P and T are pitch (as shown in Fig. 8) and taper of the threaded pipe, s and s_1 are scaling parameters, and α is the misalignment angle between centerlines of threaded pipe and casing, as shown in Fig. 9. $f(\alpha)$ is a monotonic function that characterizes the deformation change with respect to the change of α. Generally, α is extremely small; otherwise, the threaded pipe cannot be coupled. Thus, we assume that $f(\alpha)$ can be approximated by a linear function of α. Noteworthy, other latent factors that induce the quasi-periodic profiles such as pipe unstraightness can be equivalent to pipe misalignment based on error equivalence theory [22].

In this sensitivity analysis, we vary α from 0.1° to 1.5°. Signals in the thread engagement phase are generated from (14) and y_k can be represented as

$$y_k = \begin{cases} h(x_k) + \psi, & k = 1, \ldots, K_1 \\ s_2(k - c_1) + h(c_1) + \psi, & k = K_1 + 1, \ldots, K_2 \\ s_3(k - c_2) + s_2(c_2 - c_1) + h(c_1) + \psi, & \\ & k = K_2 + 1, \ldots, T \end{cases} \tag{15}$$

where ψ is Gaussian noise, which follows normal distribution $N(0, \sigma_3^2)$. x_k can be represented as $x_k = s_4 k + \vartheta$, $\vartheta \sim N(0, \sigma_4^2)$. We set $s = 100$, $T = (1/16)$, $p = 5.6$, $s_1 = 300$, $s_2 = 2000$, $s_3 = 4000$, $s_4 = 0.002, \sigma_3 = 80$, and $\sigma_4 = 0.003$, respectively, and the change point locations on x_k are $c_1 = 3.3$, $c_2 = 3.7$ in this sensitivity analysis. A total of 1000 replications are conducted for each varied α. Fig. 10 shows the detection results of three random examples by our proposed method under $\alpha = 0.5°$, 1°, and 1.5°,

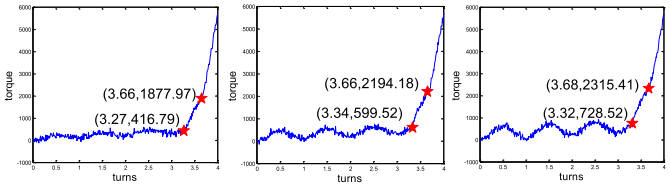

Fig. 10. Examples of change point detection in sensitivity analysis under (Left) $\alpha = 0.5°$, (Middle) $\alpha = 1°$, and (Right) $\alpha = 1.5°$.

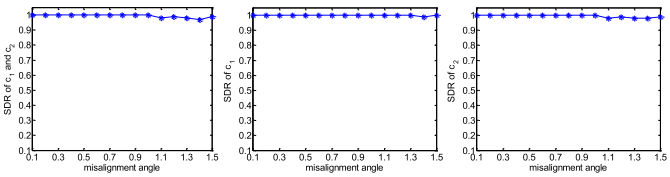

Fig. 11. SDRs of c_1 and c_2 under α from 0.1° to 1.5° with an interval of 0.1°. SDR of both (Left) c_1 and c_2, (Middle) c_1, and (Right) c_2.

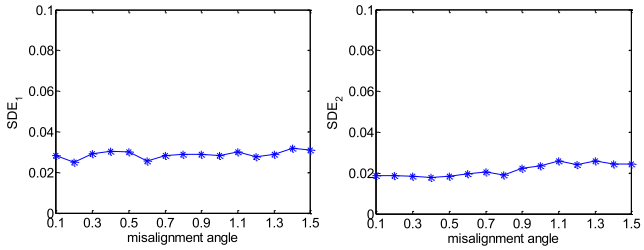

Fig. 12. SDEs of (Left) c_1 and (Right) c_2 under α from 0.1° to 1.5° with an interval of 0.1°.

respectively. Although the detected locations of change points in the x-axis are not exactly the same as the actual setting locations, the differences between our detected change points are remarkably small and meet the requirement in practice, thereby indicating that our proposed method can accurately identify change points under different misalignment situations.

To further show how the proposed method performs under different misalignment situations, in this sensitivity analysis, we use the same evaluation criteria from the aforementioned simulation studies. Figs. 11 and 12 show the detection results. The SDRs and SDEs of change point detection are consistent over the misalignment angle changes.

V. Real Case Study

Our proposed method has been applied in change point detection of real torque signals collected from one steel pipe plant. We obtain 84 samples with a pair of change points labeled by the technical engineers in the plant. All these signals have various nonlinear profiles, unequal lengths, and horizontal oscillations. The sampling frequency is 20 Hz.

We will first show the performance of our proposed method on this real data set, and then compare our proposed method with other existing methods including three-phase regression method [21], state-space model-based method [18], and sequential piecewise linear approach [17]. The engineering specifications h_1, h_2, and h_3 in sequential change point

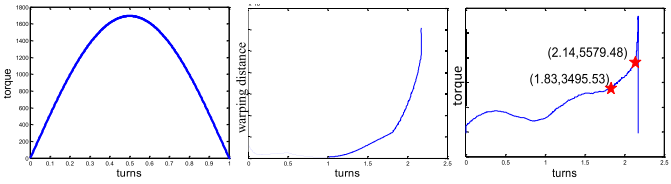

Fig. 13. Illustrations of our proposed method for one random sample. (Left) Physical basis function. (Middle) Warping distance between "physical basis function" and torque sequence. (Right) Detection results.

selection are 0.126, 0.802, and 0.126 in terms of engineering design requirements.

Fig. 13 illustrates our proposed method by one example of pipe tightening, including physical basis function, warping distance, and detected change points over torques. We also show eight typical examples with various nonlinear profiles from our 84 samples. As shown in Fig. 14, the signal lengths range from 1.24 to 5.68 screwing turns, and a variety of torque profiles can be observed. The change points that separate the critical phases of the tightening process are accurately identified from various nonlinear profiles in the torque signals by our proposed method. Owing to unequal lengths of torque signals, the speed of our proposed method depends on the length of torque signals. The calculation time for the largest length sample is 78.08 s by using MATLAB R2013a on a computer with Intel Core-i5-4210U @ 2.40 GHz processor, 4 GB of RAM, which satisfies the requirements of in-line process monitoring.

Given that the sampling frequency of the torque signal is 20 Hz, a range of screwing turns $[-0.3, 0.3]$ for the first change point and $[-0.04, 0.03]$ for the second change point are defined as the criteria for the detection power to meet the engineering requirements, thereby indicating that the tolerance of the successful detections of the two change points should be within the given two ranges, respectively. The detection results are listed in Table IV, where our proposed method achieves 100% SDR for the first change point, 98.81% SDR for the second change point, and 98.81% SDR for a pair of change points. In addition, our proposed method achieves a small SDE for each change point, which are 0.0728 for the first change point and 0.0103 for the second change point.

We first compare our proposed method with an empirical method [2], which is widely used in steel pipe plants at present. This method can only identify the second change point from torque signals. This empirical method calculates the "derivative" of torque signals and regards the first point whose slope is over the given threshold as the second change point. We use the same data set and evaluation criteria to test this method, and the detection results are listed in Table IV. The SDR of the second change point is 5.95%, which is much lower than the proposed method.

We also compare our method with three other popular change detection methods, which are three-phase regression model based on $F_{\max}$ test [21], state-space model-based method [18], and two-stage sequential piecewise linear approach [17], respectively. The same data set and evaluation criteria are applied to test these methods, and the detection

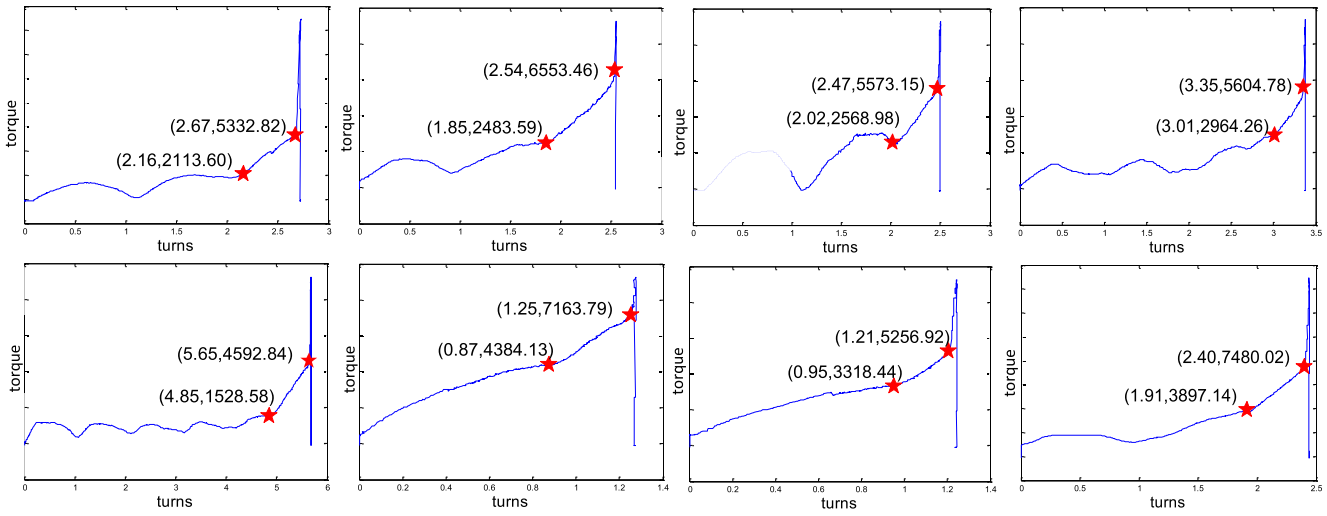

Fig. 14. Examples of change point detection in torque signals with diverse nonlinear patterns.

TABLE IV
CHANGE POINT DETECTION RESULTS OF OUR PROPOSED METHOD AND OTHER EXISTING METHODS ON THE COLLECTED TORQUE SIGNAL DATA SET FROM STEEL PLANT

Methods	SDR (%)			SDE	
	c_1	c_2	c_1 & c_2	SDE_1	SDE_2
Our Proposed Method	100.00	98.81	98.81	0.0728	0.0103
VAM method [2]	-	5.95	-	-	0.0814
Three-phase Regression [21]	32.14	95.24	30.59	0.9477	0.0564
State-space model [18]	46.43	59.52	28.57	0.8414	0.4022
Sequential Piecewise Linear [17]	66.67	94.05	60.71	0.2609	0.0224

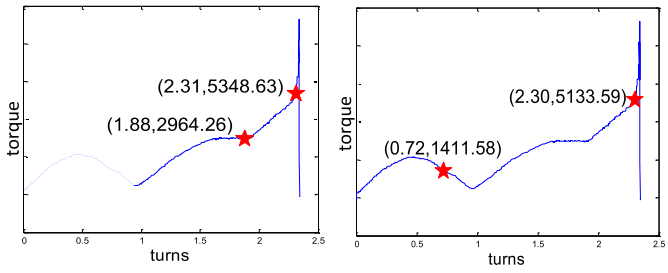

Fig. 15. Comparisons between (Left) our proposed method and (Right) three phase regression method for change point detection.

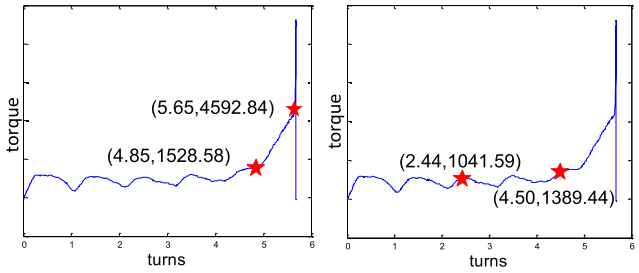

Fig. 16. Comparisons between (Left) our proposed model and (Right) method in [18] of one example in pipe tightening process.

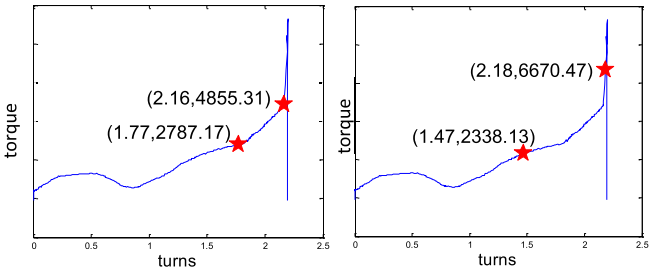

Fig. 17. Comparisons between (Left) our proposed model and (Right) method in [17] for change point detection in torque signals.

results are also listed in Table IV. Specifically, we can conclude that the SDRs of our proposed method are much higher than others for the first change point, second change point, and both the first and second change points, respectively. Figs. 15–17 show comparisons between our proposed method and the others, which indicate our proposed method is more effective for change point detection from multiple nonlinear profiles in torque signals than the other three existing change detection methods.

To better illustrate the detection results of our method and other existing methods on the same real data set, we provide a short discussion in this paragraph. As shown in Table IV, the state-space model in our previous work does not perform well in this real data set. Owing to the linear structure in the state-space model, the performance of the state estimation may be greatly deteriorated if various nonlinear profiles with similar slope as the nominal curve has. In practice, since the process condition in upstream work stage is not always stable, this leads to a large number of nonlinear profiles in the

torque signals during the connection procedure. This method shows a satisfactory detection power on the torque signals with few simple nonlinear profiles (e.g., a single quasi-periodic profile exists in the torque), but cannot effectively identify multiple change points in torque signals with various nonlinear profiles (e.g., multiple quasi-periodic profiles with varying periods and lengths). The three-phase regression method and sequential piecewise linear method perform well for the second change point but fail for the detection of sealing point. The reason is that the disastrous nonlinear profiles (especially, the quasi-periodic profiles) primarily dominate in the thread engagement phase and almost mask the sealing point, and these methods lack investigation in the generation mechanism of signal profiles.

VI. Conclusion

This paper develops a novel change point detection method for tightening process by using torque signals collected from the tightening processes. Owing to a large variety of uncertainties during the tightening process, the measured torque signals usually contain multiple quasi-periodic nonlinear profiles, thereby resulting in a considerable challenge for the accurate detection of change points in torque signals. To address this challenge, we consider engineering knowledge and propose a similarity-weighted matrix to reduce the negative effects induced by the multiple nonlinear profiles.

The numerical studies, sensitivity analysis, and real case study show that our proposed method achieves high detection power for change point detection from multiple nonlinear profiles in torque signals in terms of SDR and SDE. Furthermore, our proposed method outperforms other existing methods for change point detection, especially for the first change point detection. Notably, although the proposed method is demonstrated for the tightening process, the entire framework on change point detection can be extended or modified for applications in other manufacturing processes.

Appendix

A. Introduction of Dynamic Time Warping

We assume two time series Q and C, with the lengths n and m, respectively, where

$$Q = q_1, q_2, \ldots, q_i, \ldots, q_n \tag{16}$$

$$C = c_1, c_2, \ldots, c_j, \ldots, c_m. \tag{17}$$

To best align these two sequences using dynamic time warping, an n-by-m matrix is designed, where the (ith, jth) element of the matrix is obtained by Euclidean distance as the local distance between two elements q_i and c_j, that is, $d(q_i, c_j) = (q_i - c_j)^2$. Subsequently, a warping path W_d, which is defined as a matching index between series Q and C with a contiguous set of matrix elements, can be represented as

$$W_d = w_1, w_2, \ldots, w_f, \ldots, w_F, \max(m, n) \le F < m + n - 1 \tag{18}$$

where F is the length of the warping path. The fth element in W_d is $w_f = (i, j)$, which represents the mapping point between the ith element of time series Q and the jth element of time series C.

Three constraints are placed on the warping path. First, the warping path should begin at the start of each time series and complete at the end of these two time series, that is, the condition that $w_1 = (1, 1)$ and $w_F = (m, n)$ should be satisfied concurrently. Second, permissible steps are required to adjacent cells along the warping path. Here, the diagonal cell is also included in the adjacent cells. Specifically, if $w_f = (a, b)$ and $w_{f-1} = (a', b')$, then the relationship between a and a', b and b' should satisfy $a - a' \le 1$ and $b - b' \le 1$. Third, the point indices in the warping path W_d should be monotonically increasing. Generally, an exponential number of warping paths satisfy the aforementioned three conditions, and the one which minimizes the warping cost is the optimal warping path. The cost is defined by

$$\mathrm{DTW}(Q, C) = \min_{W_d} \left(\frac{\sum_{f=1}^{F} d(w_f)}{F} \right). \tag{19}$$

The solution of the optimal warping path can be addressed by dynamic programing, which evaluates the recurrence of the cumulative distance $\gamma(i, j)$ in the adjacent elements as follows:

$$\gamma(i, j) = d(q_i, c_j) + \min \begin{cases} \gamma(i-1, j-1) \\ \gamma(i-1, j) \\ \gamma(i, j-1). \end{cases} \tag{20}$$

B. Derivation of $\hat{\lambda}_i$ in Section III-D

Denote $\boldsymbol{W}_1 = \mathrm{diag}(\omega_1, \ldots, \omega_{c_1})$, $\boldsymbol{Y}_1 = (y_1, \ldots, y_{c_1})^T$, $\boldsymbol{W}_2 = \mathrm{diag}(\omega_{1+c_1}, \ldots, \omega_{c_2})$, $\boldsymbol{Y}_2 = (y_{1+c_1}, \ldots, y_{c_2})^T$, $\boldsymbol{W}_3 = \mathrm{diag}(\omega_{1+c_2}, \ldots, \omega_n)$, $\boldsymbol{Y}_3 = (y_{1+c_2}, \ldots, y_n)^T$,

$$\boldsymbol{X}_1 = \begin{pmatrix} 1, \ldots, 1 \\ x_1, \ldots, x_{c_1} \end{pmatrix}^T, \quad \boldsymbol{X}_2 = \begin{pmatrix} 1, \ldots, 1 \\ x_{1+c_1}, \ldots, x_{c_2} \end{pmatrix}^T,$$

$$\boldsymbol{X}_3 = \begin{pmatrix} 1, \ldots, 1 \\ x_{1+c_2}, \ldots, x_n \end{pmatrix}^T,$$

$\boldsymbol{\lambda}_i = (a_i, b_i)^{\mathrm{T}}, i = 1, 2, 3$, then WRSS in (16) can be written as $\mathrm{WRSS} = \sum_{i=1}^{3} (\boldsymbol{Y}_i - \boldsymbol{X}_i \boldsymbol{\lambda}_i)^T \boldsymbol{W}_i (\boldsymbol{Y}_i - \boldsymbol{X}_i \boldsymbol{\lambda}_i)$. Assume that there is a symmetric matrix C such that $W_i = C^T C = C C^T$, then

$$\begin{aligned} \mathrm{WRSS}(\lambda_i) &= (Y_i - X_i \lambda_i)^T C^T C (Y_i - X_i \lambda_i) \\ &= [C(Y_i - X_i \lambda_i)]^T [C(Y_i - X_i \lambda_i)]. \end{aligned}$$

Let $\tilde{Y}_i = C Y_i \tilde{X}_i = C X_i$, then

$$\begin{aligned} \mathrm{WRSS}(\lambda_i) &= (\tilde{Y}_i - \tilde{X}_i \lambda_i)^T (\tilde{Y}_i - \tilde{X}_i \lambda_i) \\ \hat{\lambda}_i &= (\tilde{X}^T \tilde{X})^{-1} \tilde{X}^T \tilde{Y} = \left(X_i^T C^T C X_i\right)^{-1} X_i^T C^T C Y_i \\ &= \left(X_i^T W_i X_i\right)^{-1} X_i^T W_i Y_i, \quad i = 1, 2, 3. \end{aligned}$$

The last equation is from the ordinary least squares in linear regression [23]. Notably, in our case, W_i forms the diagonal matrix with positive elements, so matrix C always exists. For example, $C = \mathrm{diag}(\sqrt{\omega}_1, \ldots, \sqrt{\omega}_n)$.

REFERENCES

[1] H. Xu, T. Shi, and Z. Zhi, "Theoretical analysis on makeup torque in tubing and casing premium threaded connections," *J. Southwest Petroleum Univ.*, vol. 36, no. 5, pp. 160–168, 2014.

[2] VAM Connections. (Apr. 2016). *VAM Book*. [Online]. Available: http://www.vamservices.com/Library/files/VAM%C2%AE%20Book.pdf

[3] Y. Guangjie, Y. Zhenqiang, W. Qinghua, and T. Zhentong, "Numerical and experimental distribution of temperature and stress fields in API round threaded connection," *Eng. Failure Anal.*, vol. 13, no. 8, pp. 1275–1284, 2006.

[4] *Recommended Practice on Procedures for Testing Casing and Tubing Connections*, document API RP 5C5, 2003, American Petroleum Institute, 2015.

[5] G. V. Moustakides, A. S. Polunchenko, and A. G. Tartakovsky, "A numerical approach to performance analysis of quickest change-point detection procedures," *Stat. Sinica*, vol. 21, no. 2, pp. 571–596, 2011.

[6] V. Spokoiny, "Multiscale local change point detection with applications to value-at-risk," *Ann. Stat.*, vol. 37, no. 3, pp. 1405–1436, 2009.

[7] H. Choi, H. Ombao, and B. Ray, "Sequential change-point detection methods for nonstationary time series," *Technometrics*, vol. 50, no. 1, pp. 40–52, 2012.

[8] L. R. Olsen, P. Chaudhuri, and F. Godtliebsen, "Multiscale spectral analysis for detecting short and long range change points in time series," *Comput. Stat. Data Anal.*, vol. 52, no. 7, pp. 3310–3330, 2008.

[9] Z. Kong, A. Oztekin, O. Beyca, U. J. Phatak, S. T. Bukkapatnam, and R. Komanduri, "Process performance prediction for chemical mechanical planarization (CMP) by integration of nonlinear Bayesian analysis and statistical modeling," *IEEE Trans. Semicond. Manuf.*, vol. 23, no. 2, pp. 316–327, May 2010.

[10] C. Cheng *et al.*, "Time series forecasting for nonlinear and nonstationary processes: A review and comparative study," *IIE Trans.*, vol. 47, no. 10, pp. 1053–1071, 2015.

[11] Z. Harchaoui and C. Lévy-Leduc, "Multiple change-point estimation with a total variation penalty," *J. Amer. Stat. Assoc.*, vol. 105, no. 492, pp. 1480–1493, 2012.

[12] J.-J. Jeon, J. H. Sung, and E.-S. Chung, "Abrupt change point detection of annual maximum precipitation using fused lasso," *J. Hydrol.*, vol. 538, pp. 831–841, Jul. 2016.

[13] C. Du, C.-L. M. Kao, and S. C. Kou, "Stepwise signal extraction via marginal likelihood," *J. Amer. Stat. Assoc.*, vol. 111, no. 513, pp. 314–330, 2016.

[14] X. Yue *et al.*, "Generalized wavelet shrinkage of inline Raman spectroscopy for quality monitoring of continuous manufacturing of carbon nanotube buckypaper," *IEEE Trans. Autom. Sci. Eng.*, vol. 14, no. 1, pp. 196–207, Jan. 2017.

[15] C. Zhou, K. Liu, X. Zhang, W. Zhang, and J. Shi, "An automatic process monitoring method using recurrence plot in progressive stamping processes," *IEEE Trans. Autom. Sci. Eng.*, vol. 13, no. 2, pp. 1102–1111, Apr. 2016.

[16] R. Ruehmann and G. Ruark, "Shoulder yielding detection during pipe make up," in *Proc. Offshore Technol. Conf.*, 2011, p. 11.

[17] J. Du and X. Zhang, "A critical change point detection method in threaded steel pipe connection processes using two stage sequential piecewise linear approach," in *Proc. ASME*, 2016, p. 8, Paper MSEC 2016-8757.

[18] J. Du, X. Zhang, and J. Shi, "Pairwise critical point detection using torque signals in threaded pipe connection processes," *ASME J. Manuf. Sci. Eng.*, vol. 139, no. 9, p. 091002, 2017.

[19] S. J. Chen, Q. An, Y. Zhang, and Q. Li, "Research on the calculation method of tightening torque on P-110s threaded connections," *J. Pressure Vessel Technol.*, vol. 133, no. 5, p. 051207, 2011.

[20] Y. Zhuang, L. Gao, X. Lu, B. Chen, Y. Zhou, and P. Yuan, "Make-up torque calculation and analysis of gas sealing joint," *J. East China Univ. Sci. Tech.*, vol. 41, no. 4, pp. 575–580, 2015.

[21] R. Lund and J. Reeves, "Detection of undocumented changepoints: A revision of the two-phase regression model," *J. Climate*, vol. 15, no. 17, pp. 2547–2554, 2002.

[22] H. Wang, "Error equivalence theory for manufacturing process control," Ph.D. dissertation, Dept. Ind. Manag. Syst. Eng., Univ. South Florida, Tampa, FL, USA, 2007.

[23] J. Friedman, T. Hastie, and R. Tibshirani, *The Elements of Statistical Learning*. Berlin, Germany: Springer, 2001.

[24] *Recommended Practice for Care and Use of Casing and Tubing*, document API RP 5C1, American Petroleum Institute, 1999.

[25] *Recommended Practice on Procedures for Testing Casing and Tubing Connections*, document API RP 5C5, American Petroleum Institute, 2003.

[26] E. Keogh and C. A. Ratanamahatana, "Exact indexing of dynamic time warping," *Knowl. Inf. Syst.*, vol. 7, no. 3, pp. 358–386, 2005.

[27] S. M. Pandit and S. M. Wu, *Time Series and System Analysis With Applications*. New York, NY, USA: Wiley, 1983.

[28] J. Wu, Y. Chen, S. Zhou, and X. Li, "Online steady-state detection for process control using multiple change-point models and particle filters," *IEEE Trans. Autom. Sci. Eng.*, vol. 13, no. 2, pp. 688–700, Apr. 2016.

[29] J. Wu, Y. Chen, and S. Zhou, "Online detection of steady-state operation using a multiple-change-point model and exact Bayesian inference," *IIE Trans.*, vol. 48, no. 7, pp. 599–613, 2016.

Juan Du (M'17) received the B.S. degree in composite material science and engineering from the Harbin Institute of Technology, Harbin, China, in 2014. She is currently pursuing the Ph.D. degree with the Department of Industrial Engineering and Management, Peking University, Beijing, China.

She is a Visiting Student with the H. Milton Stewart School of Industrial and Systems Engineering, Georgia Institute of Technology, Atlanta, GA, USA. Her current research interests include data analytics for process monitoring, control, and diagnosis in complex manufacturing systems.

Ms. Du is a member of ASQ, INFORMS, and IISE.

Xi Zhang (M'13) received the B.S. degree in mechanical engineering and automation from Shanghai Jiaotong University, Shanghai, China, in 2006, and the Ph.D. degree in industrial engineering from the University of South Florida, Tampa, FL, USA, 2010.

He is currently an Associate Professor with the Department of Industrial Engineering and Management, Peking University, Beijing, China. His current research interests include physical-statistical modeling and analysis for process monitoring, diagnosis, and optimization in complex dynamic systems.

Dr. Zhang is a member of INFORMS, IISE, and ASQ.

Jianjun Shi received the B.S. and M.S. degrees in electrical engineering from the Beijing Institute of Technology, Beijing, China, in 1984 and 1987, respectively, and the Ph.D. degree in mechanical engineering from the University of Michigan, Ann Arbor, MI, USA, in 1992.

He is currently the Carolyn J. Stewart Chair and a Professor with the H. Milton Stewart School of Industrial and Systems Engineering, with joint appointment in the George W. Woodruff School of Mechanical Engineering, Georgia Institute of Technology, Atlanta, GA, USA. His current research interests include the development and application of data enabled manufacturing, system informatics, advanced statistics, and control theory for the design and operational improvements of manufacturing and service systems by fusing engineering systems models with data science methods.

Dr. Shi is a Fellow of IIE, ASME, and INFORMS, an Academician of the International Academy for Quality, and a member of the U.S. National Academy of Engineering.